Conformation of Two Peptides Corresponding to Human Apolipoprotein C-I Residues 7−24 and 35−53 in the Presence of Sodium Dodecyl Sulfate by CD and NMR Spectroscopy[†,‡]

Annett Rozek, Garry W. Buchko, and Robert J. Cushley*

Department of Chemistry and Institute of Molecular Biology and Biochemistry, Simon Fraser University, Burnaby, British Columbia, Canada V5A 1S6

Received December 22, 1994; Revised Manuscript Received March 15, 1995[⊗]

ABSTRACT: Peptides corresponding to the proposed lipid-binding domains of human apolipoprotein C-I, residues 7−24 (ALDKLKEFGNTLEDKARE) and 35−53 (SAKMREWFSETFQKVKEKL), were studied by CD and two-dimensional ^{1}H NMR spectroscopy. Sodium dodecyl sulfate (SDS) was used to model the lipoprotein environment. Analysis of the CD data shows that both peptides lack well-defined structure in aqueous solution but adopt helical, ordered structures upon the addition of SDS. The helical nature of the peptides in the presence of SDS was confirmed by H^α secondary shifts. A total of 199 (apoC-I(7−24)) and 266 (apoC-I(35−53)) distance restraints were used in distance geometry and simulated annealing calculations to generate average structures for both peptides in aqueous solutions containing SDS. The backbone (N, C^α, C=O) RMSD from the average structure of an ensemble of 20 structures was 0.73 ± 0.22 and 0.48 ± 0.14 Å for apoC-I(7−24) and apoC-I(35−53), respectively. In the presence of SDS, the distance geometry and simulated annealing calculations show that both peptides adopt well-defined amphipathic helices with distinct hydrophobic and hydrophilic faces. The calculated structures are discussed relative to predicted structures. Comparing our CD and NMR results for the apoC-I fragments in SDS with CD results of others obtained in the presence of dimyristoylphosphatidylcholine indicates that SDS may be a better model of the lipoprotein environment.

The C-group of exchangeable apolipoproteins (apoC-I, apoC-II, apoC-III$_0$, apoC-III$_1$, and apoC-III$_2$) make up 40% of the proteins of VLDL[1] and are minor components of HDL. High plasma concentrations of HDL have been inversely correlated with the risk of atherosclerosis (Miller & Miller, 1975). The C-apolipoproteins transfer between classes of lipoproteins and impart particular properties to them. For instance, upon transfer from HDL to chylomicrons they delay clearance of the chylomicrons from circulating plasma (Windler & Havel, 1985). This delay has recently been shown to be due mainly to apoC-I (Weisgraber et al., 1990). The apoCs are also important regulators of the catabolism of VLDL to LDL in that they modulate LCAT, LpL, and HL activities and affect binding to receptors. The mechanism of apoC association with lipoproteins is not known. ApoC-I, a 57-residue protein (M_r = 6653), activates LCAT about 70% as effectively as apoA-I. LCAT is an enzyme which transesterifies an *sn*-2 fatty acid from phosphatidylcholine to cholesterol to yield cholesteryl esters (Fielding et al., 1972; Soutar et al., 1975; Albers et al., 1979; Matz & Jonas, 1982). ApoC-I probably becomes important for people suffering HDL deficiency diseases. For example, patients with Tangiers' disease, apoA-I mutations, or apoA-I/apoC-III deficiencies all have below average levels of apoA-I but exhibit normal LCAT activity (Sweeny & Jonas, 1985), and therefore, apoC-I may be the active factor. ApoC-I has a high content of lysine (16 mol %) which makes it very soluble at acid pH and barely mobile in alkaline polyacrylamide gel electrophoresis. It contains no histidine, tyrosine, or cysteine and no carbohydrate. ApoC-I undergoes self-association in aqueous solution, and the conformational changes that accompany the self-association are dramatic (Osborne et al., 1977). Below pH 3 apoC-I does not self-associate.

The plasma apolipoproteins are characterized by repeating amino acid motifs of 11 or 22 residues which, based upon predictions from primary sequences, may form an amphipathic helical structure when associated with lipid (Segrest et al., 1990). By definition, an amphipathic helix possesses polar and nonpolar faces oriented on opposite sides of the long axis of an α-helix. In a phospholipid environment the model predicts that the hydrophobic amino acid residues on the nonpolar face interact with the acyl chains of the lipid while the hydrophilic amino acid residues on the polar face are exposed to the aqueous medium. On the basis of physical−chemical and structural properties, Segrest et al.

[†] This work was supported by the Heart and Stroke Foundation of BC and Yukon and the Natural Science and Engineering Research Council of Canada.

[‡] Brookhaven Protein Data Bank identification numbers: 1ALF for apoC-I(35−53); 1ALE for apoC-I(7−24).

* Correspondence should be addressed to this author at the Institute of Molecular Biology and Biochemistry, Simon Fraser University, Burnaby, British Columbia, Canada V5A 1S6. Telephone: 604-291-4230; Fax: 604-291-5583; E-mail: cushley@sfu.ca.

[⊗] Abstract published in *Advance ACS Abstracts,* May 1, 1995.

[1] Abbreviations: VLDL, very low density lipoprotein; HDL, high density lipoprotein; LDL, low density lipoprotein; LCAT, lecithin−cholesterol acyl transferase; LpL lipoprotein lipase; HL, hepatic lipase; CD, circular dichroism; NMR, nuclear magnetic resonance; SDS, sodium dodecyl sulfate; NOESY, nuclear Overhauser enhancement spectroscopy; HPLC, high-performance liquid chromatography; TOCSY, total correlation spectroscopy; DQF-COSY, double-quantum-filtered correlated spectroscopy; CCA, convex constraint analysis; NOE, nuclear Overhauser effect; RMSD, root mean square deviation; DPC, dodecylphosphocholine; DMPC, dimyristoylphosphatidylcholine; EYL, egg yolk lecithin.

0006-2960/95/0434-7401$09.00/0

(1990) have grouped amphipathic helices into seven distinct classes (A, H, L, G, K, C, and M) with subdivisions. ApoC-I sequences 7−32 and 33−53 are predicted to fall into the A_2 amphipathic helix class where the positively charged amino acid residues are located at the polar−nonpolar interface and the negatively charged amino acid residues are located at the center of the polar face (Segrest et al., 1990, 1992; Brasseur et al., 1992).

In order to understand apolipoprotein function, a number of studies were initiated using model peptides, some with no sequence homology to any lipoprotein. The criteria for such peptides were a minimum length (>18 residues), a high hydrophobicity, and an ability to bind strongly and form a stable amphipathic structure when associated with lipid (Fukushima et al., 1980; Pownall et al., 1980; Epand et al., 1989). For example, Yokoyama et al. (1980) synthesized a 22 amino acid amphipathic peptide which, relative to apoC-I, stimulated the phospholipase activity of LCAT up to 70%, but, only stimulated the esterifying activity of LCAT by 26%. Pownall et al. (1980) prepared a 20-residue lipid-associating peptide (LAP-20) containing a single lipid-binding domain which activated transacylation as well as apoC-I. Both studies concluded that activation resulted from interaction of the peptide with the phospholipid rather than via an interaction of the peptide with the enzyme. Subbarao et al. (1988) demonstrated that a 30-residue hydrophobic peptide with no positive charges (GALA) activated LCAT in the presence of dimyristoylphosphatidylcholine and concluded that lipid association, but not positive charges, was required to activate LCAT. While these results with model peptides have been far from satisfactory, the consensus has been that association with lipid is a necessary, but by itself not a sufficient, criterion for enzyme activation.

To further understand the conformational changes that occur upon the association of apolipoprotein with lipid, we have obtained two chemically synthesized peptides representing the amino (7−24) and carboxyl (35−53) ends of human apolipoprotein C-I. Both peptides are predicted to adopt class A_2 amphipathic conformations (Segrest et al., 1992; Brasseur et al., 1992) and are segments of larger fragments of apoC-I (1−38 and 32−57) which have been shown to have an affinity for lipid (Jackson et al., 1974; Sparrow et al., 1977). Sodium dodecyl sulfate, a commonly used agent to model membranes, was chosen to model the lipoprotein environment. Compared to large native lipoprotein complexes, smaller peptide/SDS complexes reorientate fast enough on the NMR time scale to give narrow NMR resonances which yield information about the bound conformation.

The amount of helical structure adopted by our peptides in the absence and in the presence of increasing concentrations of sodium dodecyl sulfate was estimated by circular dichroism. Two-dimensional ^{1}H NMR studies were performed in the presence of SDS-d_{25} at a molar ratio of peptide to SDS of 1:40. The helical content was estimated by H^α chemical shift analysis. Using distance restraints obtained from NOESY data, average structures for both peptides in SDS were obtained with distance geometry and simulated annealing calculations. A comparison is made between the structures we calculated for both apoC-I fragments in the presence of SDS and structures predicted from theoretical calculations. The biological significance of the peptide structures we observed in the model lipid environment is discussed in relation to the native apolipoprotein C-I secondary structure.

MATERIALS AND METHODS

Human apolipoprotein C-I peptides corresponding to residues 7−24 and 35−53 were synthesized by Dr. Ian Clark-Lewis (University of British Columbia) using solid-phase methods (Clark-Lewis et al., 1986). SDS was purchased from BDH Chemicals Ltd.; perdeuterated SDS (SDS-d_{25}) was purchased from Cambridge Isotope Laboratories Inc.; D_2O was purchased from STOHLER/KOR Stable Isotopes Inc. Insight II (v.2.3.0), NMRchitect, DGII, and FELIX (v.2.1, Hare Research Inc.) software were generously provided by Biosym Technologies Inc. (San Diego, CA).

Circular Dichroism Spectroscopy. CD spectra were obtained on a Jasco J710 spectropolarimeter calibrated using ammonium *d*-(+)-camphorsulfonate. The measurements were performed in a quartz cell of 0.02 cm path length at 25 °C using a Neslab RTE-110 circulating water bath. The peptide concentrations were 0.5 mM, at a pH between 3.8 and 6.0. Spectra were the average of 2 consecutive scans from 260 to 190 nm recorded with a bandwidth of 0.5 nm, a scan rate of 10 nm/min, and a time constant of 0.25 s. Following base-line correction and noise reduction, the observed ellipticities were converted to mean residue ellipticities, $[\theta]$, in units of deg·cm^2/dmol.

NMR Spectroscopy. Samples (5 mM) for ^{1}H NMR spectroscopy were prepared either in 90% H_2O/10% D_2O or in 99.9% D_2O by dissolving the peptides in 600 μL of 200 mM SDS-d_{25}. The pH was adjusted to 4.8 ± 0.1 with the addition of 0.1 M NaOH (pH meter readings uncorrected for the deuterium isotope effect). Samples were allowed to equilibrate at room temperature in the dark for a minimum of 24 h before collecting spectra.

NMR experiments were run on a Bruker AMX spectrometer operating at 600.13 MHz. Two-dimensional TOCSY (Braunschweiler & Ernst, 1983; Bax & Davis, 1985), NOESY (Jeener et al., 1979), and DQF-COSY (Rance et al., 1983) spectra were recorded at 37 °C in the phase sensitive mode using time-proportional phase incrementation (TPPI) (Redfield & Kunz, 1975). A recycle delay of 2 s and a spectral width of 6024 (apoC-I(7−24)) and 7246 (apoC-I(35−53)) Hz were employed to collect 768−900 t_1 increments with 32 transients in 2K data points. The water was suppressed in the TOCSY and NOESY experiments using the WATERGATE technique (Piotto et al., 1992) which employed the 3-9-19 pulse sequence (Sklenár et al., 1993). In the DQF-COSY experiments obtained in 99.9% D_2O the residual HDO signal was suppressed by presaturation during the recycling delay. A 75 ms mixing time and 2.5 ms trim pulse was used in the MLEV-17 spin-locking sequence of the TOCSY experiments. NOESY data were recorded using mixing times of 50, 75, 100, and 150 ms.

Spectra were processed using UXNMR on a X32 workstation (Bruker) or by using the FELIX program on an Indigo2 computer (Silicon Graphics Inc.). Prior to Fourier transformation, the data were zero-filled to generate a 2K × 2K matrix and apodized by a 60° shifted sine-bell (FELIX) or a 90° shifted quadratic sine-bell (UXNMR) window function in both dimensions. Base-line corrections with a fifth-order polynomial function were applied to all processed spectra in both dimensions. Chemical shifts were referenced to external 4,4-dimethyl-4-silapentane-1-sulfonate (DSS, 0 ppm).

Structure Calculations. Three-dimensional structures were calculated from the NOE distance data (FELIX) using the distance geometry program (DGII) of InsightII.

Initial distance restraints were obtained by classifying the peak volumes of the 100 ms NOESY spectra of apoC-I(7−24) and 150 ms NOESY spectra of apoC-I(35−53) into strong (1.80−2.50 Å), medium (2.51−3.50 Å), and weak (3.51−5.00 Å) ranges. The upper bound of restraints involving nonresolvable methylene or methyl protons was adjusted by the addition of 1.0 and 1.5 Å, respectively, using the NMR-Refine module of InsightII. Nonresolvable methyl groups were adjusted by the addition of 2.4 Å to the upper bound of pertinent restraints. The same program was used to float correct resolvable, but nonstereospecifically assignable, methylene protons and methyl groups.

The distance geometry calculations consisted of three steps: smoothing, embedding, and optimization—the latter step based on simulated annealing and energy minimization of the annealed structures with a conjugated gradient (Havel, 1991). The CVFF forcefield was used with the upper and lower force constant set at 10.0 kcal/(mol·Å^2) and the maximum force constant set at 100.0 kcal/(mol·Å^2) for all constraints. Relatively low force constants were chosen to allow maximum freedom in the process of simulated annealing. Smoothing of distance bounds was done starting with a nonminimized right-handed α-helix in the sequential tetrangle mode. Coordinates were embedded in four dimensions starting from randomly chosen points in the distance limits matrix. In the simulated annealing schedule the embedded structure was heated to a maximum "temperature" of 200 K. This is defined as the average kinetic energy per degree of freedom, K_{ini} (Havel, 1991), and was achieved by increasing the energy by a factor of 2 at each step. Then, the system was gradually cooled to 0 K over 10 000 steps of 0.2 ps duration. The fail level was set below the final error of simulated annealing which reflects chirality, distance, and hard sphere contact errors. This resulted in the mirror image of the embedded structures being reannealed. Between 10 and 20 structures were generated, and distance violations greater than 0.1 Å were compiled and examined. The restraint range of these violations was either widened or eliminated to reflect uncertainty in the distance classification or incorrect integration of cross-peaks due to spectral overlap. The procedure was repeated until no distance violations greater than 0.05 Å were observed. When no further improvement could be obtained, the fail level was set above the optimization error (<0.05) to effect the execution of a conjugated gradient minimization of the structures. In the end, a total of 199 (apoC-I(7−24)) and 266 (apoC-I(35−53)) restraints were used in the final calculation of the structures.

RESULTS

CD Spectroscopy. The CD spectra from a titration of a 0.5 mM aqueous solution of apoC-I fragments 7−24 and 35−53 with SDS are shown in Figure 1. In the absence of SDS the CD spectra for both fragments show a strong negative band near 200 nm and a weak band around 220 nm which characterize peptides that lack a well-defined secondary structure (Woody, 1992). In both cases there was no observable change in the spectra over the pH range 3−11.

The addition of SDS effected changes in the CD spectra which suggested an increase in ordered secondary structure.

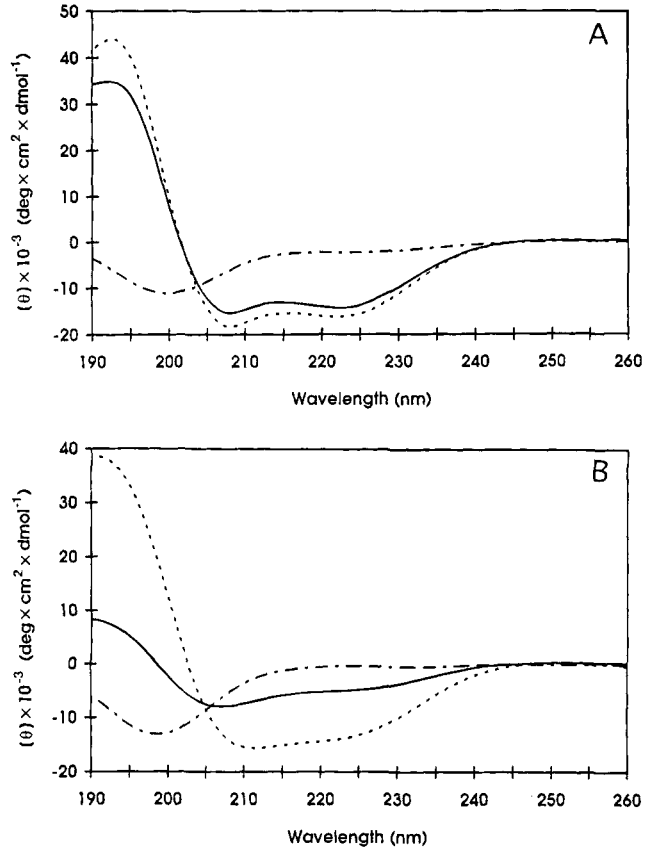

FIGURE 1: Circular dichroism spectra of apoC-I(7−24) (A) and apoC-I(35−53) (B) (0.5 mM) at 288 K in aqueous solution and at various SDS concentrations: no SDS (dashed), 5 mM SDS (A) and 0.75 mM SDS (B) (solid), and 20 mM SDS (dotted).

Spectra for fragment 7−24 are not presented in Figure 1 below a peptide:SDS ratio of 1:10 (mole:mole) due to the formation of a precipitate. At a peptide:SDS ratio of 1:10 or greater the precipitate went back into solution. A similar phenomenon was observed for apoC-I(35−53) except that this precipitate would redissolve after a few minutes of agitation. O'Neil and Sykes (1989) made similar observations upon titrating a tripeptide with lithium dodecyl sulfate and suggested the phenomenon was due to the formation of a salt between the anionic detergent and the cationic peptide. Above a peptide:SDS ratio of 1:10 for fragment 35−53 and 1:20 for fragment 7−24, no further changes were observed in the CD spectra, suggesting that the peptides were completely associated with the SDS in a micelle-bound state (Bairaktari et al., 1990). The CD spectra of the peptides in the lipid complexes are highlighted by a double minimum at 222 and 208−210 nm and a substantial maximum at 191−193 nm. Such features are indicative of a helical conformation (Holzwarth & Doty, 1965).

To quantify the amount of peptide present in the helical state, the CD spectra were deconvoluted using convex constraint analysis (CCA) (Perczel et al., 1992), and the results are presented in Table 1. The absolute percentages of secondary structure obtained by such analyses will vary depending on the weighing of secondary structures contributing to the spectra used in the basis set. However, the CCA results do illustrate trends and show an increase in helical secondary structure of both peptides as the SDS concentration is increased. Similar observations were made upon the titration of other peptides with SDS (Wu & Yang, 1978;

Table 1: α-Helical Content and Helical Parameters R1 and R2 for Human Apolipoprotein C-I Fragments 7−24 and 35−53 in the Presence of Various Ratios of SDS[a]

peptide	peptide:SDS	% α-helix CD[b]	% α-helix NMR[c]	R1[d]	R2[d]
(7−24)	1:0	0		0.52	0.14
(7−24)	1:10	59		−2.27	0.93
(7−24)	1:40	64	69	−2.41	0.89
(35−53)	1:0	4		0.48	0.30
(35−53)	1:1.5	21		−1.05	0.63
(35−53)	1:40	54	99	−2.51	0.92

[a] CD data collected in H_2O, pH 3.8−6.0, at 25 °C. Variation of the pH over the range 3.0−7.0 had no effect on the spectra. [b] Calculated using convex constraint analysis (CCA) (Perczel et al., 1992). [c] Calculated from the H^α chemical shifts according to Rizo et al. (1993) $(\delta H^\alpha_{\text{random coil}} - \delta H^\alpha_{\text{obsd}})$/no. of residues)/0.35. [d] Calculated as described by Rizo et al. (1993). R1 is the ratio between the intensity of the maximum between 190 and 195 nm and the intensity of the minimum between 200 and 210 nm. R2 is the ratio between the intensity of the minimum near 222 nm and the intensity of the minimum between 200 and 210 nm.

Bairaktari et al., 1990). Because the calculated mean molar ellipticity values are sensitive to other factors (Hennessey & Johnson, 1982; Sarver & Krueger, 1991), the CD data were also analyzed using two parameters, R1 and R2, which are independent of inaccuracies in determined peptide concentrations as well as those caused by small shifts in wavelength (Bruch et al., 1991). R1 is the ratio of the intensity of the maximum between 190 and 195 nm and the intensity of the minimum between 200 and 210 nm. R2 is the ratio of the intensity of the minimum near 222 nm and the intensity of the minimum between 200 and 210 nm. For a random structure R1 is positive and R2 is close to 0. On the other hand, in a highly helical state, R1 will be close to −2 and R2 will approach 1 (Bruch et al., 1991; Rizo et al., 1993). Such parameters, tabulated in Table 1, also show an increase in the helical secondary structure of both fragments as the SDS concentration is increased.

Proton Resonance Assignments and Secondary Shifts. Assignment of all the proton resonances for both peptides in SDS was accomplished using standard NMR procedures (Wüthrich, 1986). TOCSY spectra were used to identify spin systems, and NOESY spectra were used to obtain interresidue connectivities and to distinguish between equivalent spin systems. Assignment of side-chain resonances was confirmed from DQF-COSY spectra. Due to severe resonance overlap of the aromatic protons of Trp_{41} and Phe_{42} at 37 °C, it was necessary to obtain a TOCSY and DQF-COSY spectrum for apoC-I(35−53) at 42 °C. The higher temperature resulted in the separation of resonances which overlapped at 37 °C, allowing for unambiguous assignment of the Trp_{41} and Phe_{42} aromatic proton resonances. Significant overlap of the Glu_{13}, Leu_{18}, Asp_{20}, and Ala_{22} H^N resonances of apoC-I(7−24) made assignment of the corresponding H^α resonances difficult. Fortunately, it was possible to assign H^N_i−H^N_{i+1} NOESY cross-peaks on the basis of NOE connectivities to neighboring amino acids with unique spin systems. The H^α_i−H^N_{i+1} NOE cross-peaks were then used to assign the H^α chemical shifts. The proton chemical shifts for apoC-I(7−24) and apoC-I(35−53) in SDS-d_{25} micellar complexes are summarized in Tables 2 and 3, respectively.

Using the data tabulated in Tables 2 and 3, it is possible to calculate secondary shifts; the difference in proton chemical shifts for an amino acid residue in a secondary conformation (α-helix, β-sheet, or turn/bend) and in an unstructured (random coil) conformation. The H^α resonances of residues in an α-helix conformation tend to experience an upfield shift with respect to random coil chemical shift values. On the other hand, the H^α resonances of residues in a β-sheet conformation tend to experience a downfield shift with respect to random coil chemical shift values (Wishart et al., 1991). Secondary shifts were calculated by subtracting the measured H^α chemical shifts of the two apoC-I peptides in SDS-d_{25} complexes from the corresponding random coil values obtained by Wüthrich (1986). A semiquanititative estimation of the helical content of the two apoC-I peptides in SDS-d_{25} complexes is obtained by dividing the average H^α secondary shift by 0.35, the average upfield H^α shift observed in the amino acid residues of proteins in an α-helical conformation (Rizo et al., 1993). The results,

Table 2: ^1H Chemical Shifts (ppm)[a] of Human Apolipoprotein C-I(7−24) in SDS Micelles[b] in 90% H_2O/10% D_2O, pH 4.8, 37 °C

residue	H^N	H^α	H^β	H^γ	others
Ala-7		4.20	1.57		
Leu-8	8.70	4.47	1.96, 1.73	1.67	H^δ 0.95
Asp-9	8.20	4.18	2.65		
Lys-10	8.34	4.12	1.97, 1.75	1.55, 1.43	H^δ 1.71, H^ϵ 3.01
Leu-11	7.51	4.12	1.74	1.74	H^δ 0.99, 0.91
Lys-12	8.09	3.94	1.95, 1.88	1.63, 1.39	H^δ 1.75, H^ϵ 2.98
Glu-13	7.90	4.16	2.19	2.53, 2.47	
Phe-14	8.23	4.48	3.31, 3.20		2,6H 7.22, 3,4,5H 7.17
Gly-15	8.72	3.73, 3.58			
Asn-16	8.22	4.43	2.92, 2.82		ϵNH_2 6.77, 7.38
Thr-17	7.99	3.99	4.35	1.24	
Leu-18	7.90	3.92	1.69, 1.49	1.42	H^δ 0.73
Glu-19	8.12	3.92	2.14	2.54, 2.40	
Asp-20	7.91	4.48	2.92, 2.83		
Lys-21	7.80	4.16	1.90	1.51	H^δ 1.67, H^ϵ 2.96
Ala-22	7.91	4.25	1.44		
Arg-23	7.73	4.37	1.95, 1.81	1.67	H^δ 3.19, ϵNH 7.08
Glu-24	7.68	4.19	2.11, 1.99	2.44, 2.15	

[a] Chemical shifts are relative to DSS (0.00 ppm). [b] Peptide to SDS ratio 1:40.

Table 3: ^1H Chemical Shifts (ppm)[a] of Human Apolipoprotein C-I(35−53) in SDS Micelles[b] in 90% H_2O/10% D_2O, pH 4.8, 37 °C

residue	H^N	H^α	H^β	H^γ	others
Ser-35		4.26	4.09		
Ala-36	8.70	4.43	1.48		
Lys-37	8.18	4.18	1.84, 1.77	1.45, 1.39	H^δ 1.71, H^ϵ 3.00
Met-38	8.08	4.33	2.22, 2.11	2.60, 2.52	H^ϵ 1.95
Arg-39	7.97	4.11	2.00	1.80, 1.71	H^δ 3.26, ϵNH 7.19
Glu-40	8.05	4.18	2.18	2.47	
Trp-41	8.22	4.25	3.35		NH 9.79, 2H 7.24, 5H 7.08, 7H 7.32, 4,6H 7.22
Phe-42	8.80	3.92	3.27, 3.12		2,6H 7.33, 3,4,5H 6.98
Ser-43	8.30	4.18	4.12, 4.08		
Glu-44	8.21	4.07	2.12, 2.00	2.57, 2.45	
Thr-45	8.09	3.57	3.51	0.85	
Phe-46	8.62	4.09	3.13, 3.01		2,6H 7.13, 3,4,5H 7.24
Gln-47	7.73	3.75	2.12	2.53	ϵNH_2 7.39, 6.80
Lys-48	7.54	4.00	1.98, 1.86	1.41	H^δ 1.60, 1.71, H^ϵ 2.92
Val-49	7.89	3.57	2.08	0.98, 0.87	
Lys-50	7.98	3.71	1.60, 1.53	1.21	H^δ 1.50, 1.45, H^ϵ 2.83, 2.78
Glu-51	7.47	4.11	2.11	2.54, 2.45	
Lys-52	7.64	4.27	1.95, 1.91	1.52	H^δ 1.68, H^ϵ 3.01, 2.96
Leu-53	7.36	4.31	1.71, 1.64	1.80	H^δ 0.86, 0.84

[a] Chemical shifts are relative to DSS (0.00 ppm). [b] Peptide to SDS ratio 1:40.

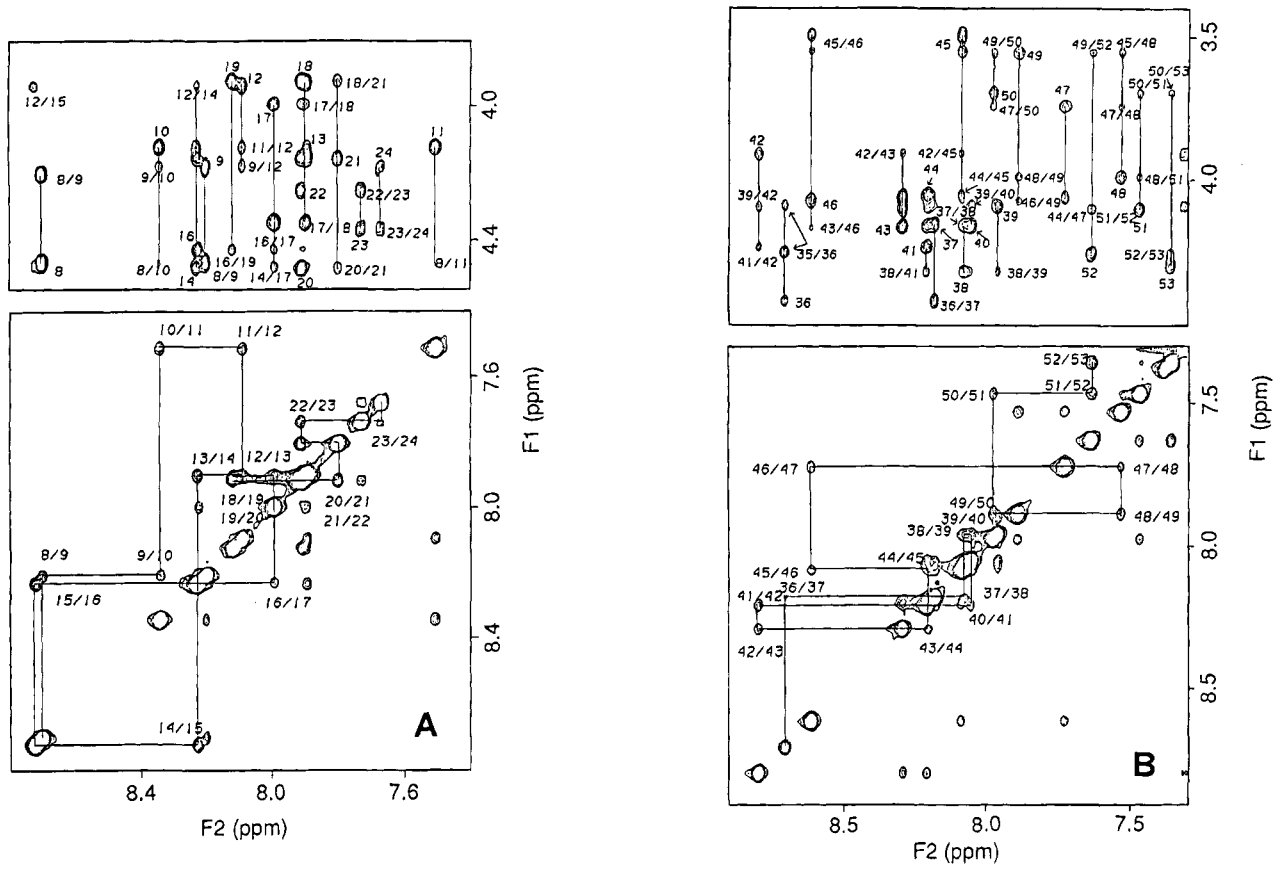

FIGURE 2: H^N-H^N and $H^\alpha-H^N$ regions of the 600-MHz NOESY spectra (τ_m = 150 ms) of apoC-I(7−24) (A) and apoC-I(35−53) (B): 5 mM peptide, 200 mM SDS, 90% H_2O/10% D_2O, pH 4.8, 37 °C. The intraresidue, sequential, and selected medium-range assignments are labeled.

tabulated in Table 1, agree with the CD data and show that both apoC-I peptides adopt a helical conformation in SDS micelles. A more detailed examination shows that the H^α secondary shifts of the two residues at the N- and C-termini approach zero in both peptides, suggesting a fraying at both ends.

Interresidue NOEs and Secondary Structure. A qualitative indication of the secondary structure of a protein is provided by the magnitude and pattern of the interresidue nuclear Overhauser effects (Wüthrich, 1986). NOESY spectra highlighting the H^N-H^N and $H^\alpha-H^N$ regions of apoC-I(7−24) and apoC-I(35−53) are presented in Figure 2 and show strong and medium, and in most cases well resolved, sequential $H^N_i-H^N_{i+1}$ and $H^\alpha_i-H^N_{i+1}$ cross-peaks. Also observed for both peptides are many medium and weak $H^N_i-H^N_{i+2}$, $H^N_i-H^N_{i+3}$, $H^\alpha_i-H^N_{i+3}$, $H^\alpha_i-H^\beta_{i+3}$, and $H^\alpha_i-H^N_{i+4}$ NOE cross-peaks, as summarized in Figure 3. The presence of strong to medium $(i)-(i+1)$ and medium to weak $(i)-(i+2)$, $(i)-(i+3)$, and $(i)-(i+4)$ NOE contacts throughout both structures suggests that they both adopt highly helical conformations when bound to SDS (Wüthrich et al., 1984; Wüthrich, 1986) in accord with the CD and secondary shift analyses.

Three-Dimensional Structure Calculations. Based on the CD data, H^α secondary shifts, and NOE connectivity patterns for both apoC-I(7−24) and apoC-I(35−53), a right-handed α-helix was chosen as the starting structure for the distance geometry and simulated annealing calculations. Figure 4 shows 19 out of 20 structures calculated for apoC-I(7−24) and 20 out of 20 structures calculated for apoC-I(35−53). In the figure the $N-C^\alpha-C{=}O$ backbone atoms are drawn with residues 9−22 and 37−51 superimposed. ApoC-I(7−24) adopts a helical structure from residues 9−22 (77%) while apoC-I(35−53) adopts a helical structure from residues 39−51 (68%). Dynamic fraying occurs at both ends of the peptides and is most pronounced at the C-terminal of apoC-I(7−24). We suggest that the effect is due to unfavorable electrostatic interactions between the helix macrodipole and the charges at the peptide termini (Shoemaker et al., 1987). The quality of the final structures is apparent from the pairwise RMSDs to the mean structure (Figure 5 and Table 4). In general, the pairwise RMSD per residue never rises above 0.2 Å for the backbone atoms and 1.1 Å for all atoms. The RMSD calculations reveal better convergence for the calculated structures for apoC-I(35−53) over apoC-I(7−24), and this likely reflects the greater number of distance restraints used in the distance geometry calculations for apoC-I(35−53), 266 versus 199.

DISCUSSION

The helical nature of both peptides in the presence of SDS, as suggested by analysis of the CD data, was confirmed by the ^1H NMR data. The H^α secondary shifts (Table 1) indicated that more than two-thirds of both peptides adopted a helical structure. Likewise, the magnitude and pattern of the interresidue NOEs (Figures 2 and 3) were characteristic of a helical conformation (Wüthrich et al., 1984; Wüthrich, 1986). The NMR data are also consistent with the peptides associating with SDS as monomers. First, the linewidths determined from one-dimensional spectra were too broad to obtain $H^\alpha-H^N$ coupling constants, indicating an increase in molecular weight due to an association with SDS (Rizo et

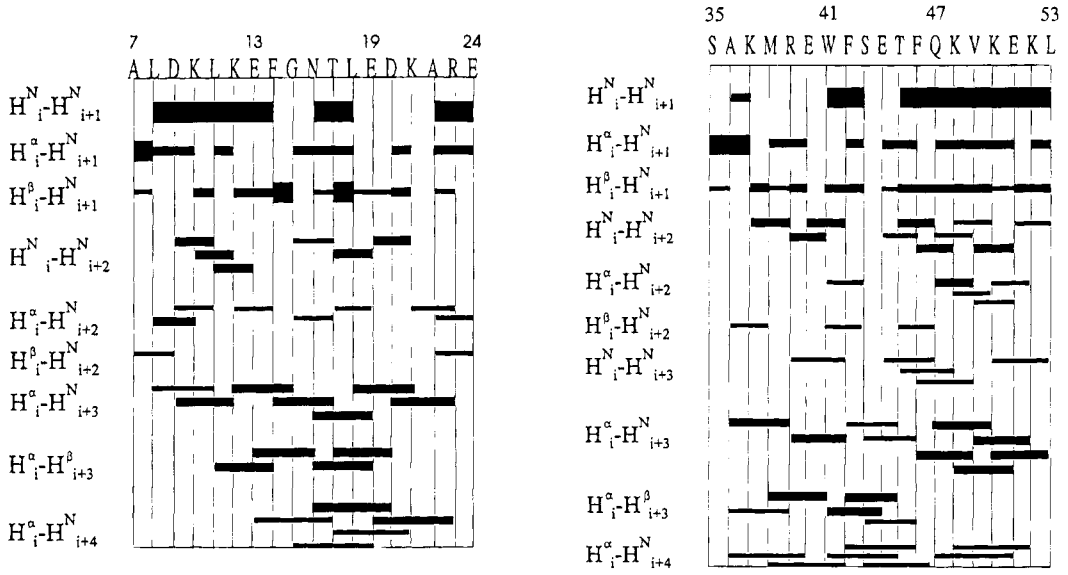

FIGURE 3: Summary of the sequential and medium-range NOEs observed for apoC-I(7−24) and apoC-I(35−53) in an aqueous solution of SDS at a mixing time of 100 and 150 ms, respectively. Classification of NOE intensities into strong, medium, and weak is indicated by the height of the bars.

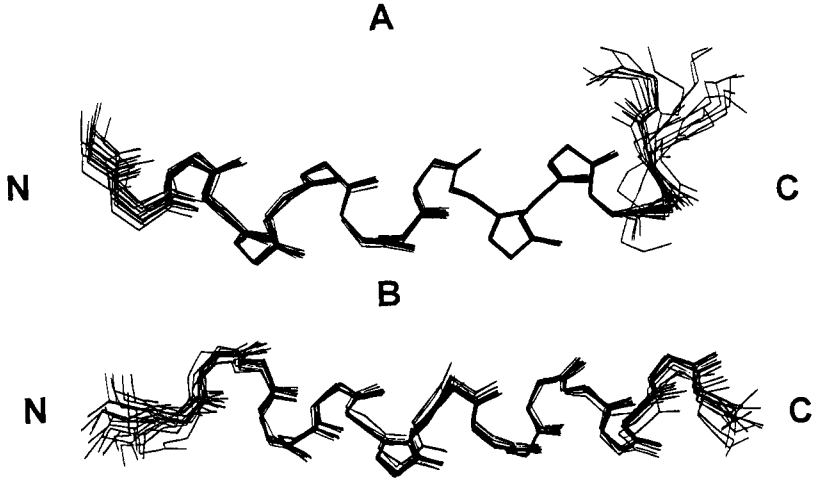

FIGURE 4: Conformational ensembles of calculated structures for apoC-I(7−24) (A) and apoC-I(35−53) (B). The backbone atoms (N−C^α−C=O) of residues 9−22 for apoC-I(7−24) and residues 37−51 for apoC-I(35−53) have been superimposed.

al., 1993; Henry & Sykes, 1994). Second, well resolved TOCSY and NOESY data (Figure 2) were collected, and all the cross-peaks could be assigned to one species (Tables 2 and 3).

Detailed three-dimensional structures were obtained for both peptides in the presence of SDS using distance geometry and simulated annealing calculations. The calculated structures show that the side chains of both peptides are generally located in three distinct regions, hydrophobic, hydrophilic, and interfacial. The aromatic residues are observed perpendicular to the plane of the hydrophobic face where they may interdigitate into the SDS dodecyl chains. The polarizable Trp_{41} in apoC-I(35−53) lies at the hydrophobic−hydrophilic interface, with the hydrophobic six-membered ring orientated toward the hydrophobic face and the imino group intruding into the hydrophilic face. The majority of the positively charged amino acid residues are located at the hydrophobic−hydrophilic interface, and the majority of the negatively charged amino acid residues are located at the center of the hydrophilic face. The orientation of the peptide side chains fits the basic description of a class A_2 amphipathic helix (Segrest et al., 1990, 1992; Brasseur et al., 1992).

One predicted feature of an A_2 amphipathic helix is a "snorkeling" of its basic amino acid side chains located at the polar−nonpolar interface (Segrest et al., 1990, 1992). In such a model the lysine and arginine residues are orientated with the side chains aligned along the edge of the hydrophobic face and the positively charged head groups extended into the hydrophilic face. While the calculated structures for both peptides show that all the basic residues, except Arg_{39} (apoC-I(35−53)), are at the interface, only Lys_{12} (apoC-I(7−24)) and Lys_{50} (apoC-I(35−53)) truly "snorkel". Consequently, this effect proposed by Segrest et al. (1990, 1992) may not be a universal characteristic of A_2 amphipathic helices.

α-Helical structures are stabilized by 2−5 kcal/mol per intramolecular hydrogen bond between backbone amide and backbone carbonyl groups four residues apart. In a perfect α-helix the hydrogen bond distance is 2.06 ± 0.16 Å ($H^N\cdots O$) and the $N-H^N\cdots O$ bond angle is 155 ± 11° (Baker & Hubbard, 1984). If apoC-I(7−24) and apoC-I(35−53) form perfect α-helices from the amino to carboxyl end, they are predicted to contain 14 and 15 such hydrogen bonds, respectively. In the calculated structures for apoC-I(7−24)

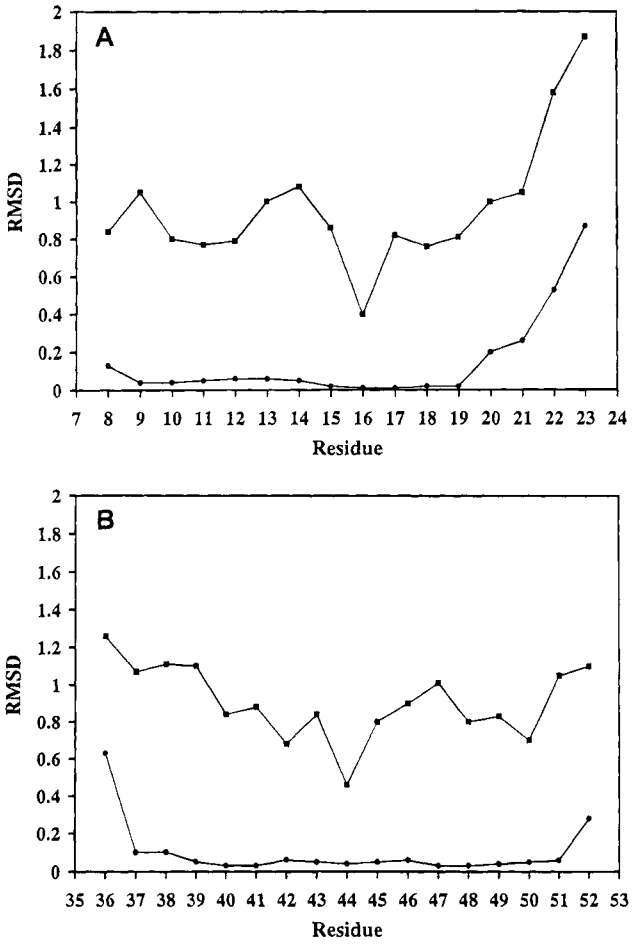

FIGURE 5: Plots of the mean pairwise RMSDs to the mean structure for each residue of apoC-I(7−24) (A) and apoC-I(35−53) (B): backbone atoms (N−C^{α}−C=O) (closed circles); all atoms (closed squares). The plots were generated by moving a window of three residues along the sequence and plotting the mean pairwise RMSD (Å) over the central residue.

Table 4: RMS Differences (Å) for Final Sets of Calculated Structures[a] of ApoC-I(7−24) and ApoC-I(35−53)

	apo C-I(7−24)	apo C-I(35−53)
all atoms:	7−24: 1.49 ± 0.27	35−53: 1.19 ± 0.18
	9−22: 1.02 ± 0.12	37−51: 1.07 ± 0.17
backbone (N, C^{α}, C=O)	7−24: 0.73 ± 0.22	35−53: 0.48 ± 0.14
	9−22: 0.23 ± 0.10	37−51: 0.23 ± 0.11

[a] 20 out of 20 calculated structures.

and apoC-I(35−53) the N−H^{N}···O atoms are in a position to form 6 and 5 hydrogen bonds, respectively, that meet the following conditions: (*i*)−(*i*+4), N−H^{N}···O bond angle between 120° and 180°, H^{N}···O distance <2.5 Å. If the above criteria are relaxed to include H^{N}···O distances that are less than 3.0 Å, then 10 and 11 hydrogen bonds may exist in apoC-I(7−24) and apoC-I(35−53), respectively. Therefore, it is likely that the helical structures of both peptides are stabilized by the formation of intramolecular hydrogen bonds.

α-Helical structures are also stabilized by up to 6 kcal/mol per intramolecular salt bridge formed by the electrostatic interaction between oppositely charged side chains that are three or four residues apart (Merutka & Stellwagen, 1991; Lyu et al., 1992; Scholtz et al., 1993). Such ion pairs, identified by X-ray crystallography, are separated by less than 3.5 Å (N···O) (Baker & Hubbard, 1984). ApoC-I(7−24) has five potential salt bridges involving every charged residue, Asp_9−Lys_{12}, Lys_{10}−Glu_{13}, Glu_{19}−Arg_{23}, Asp_{20}−Arg_{23}, and Lys_{21}−Glu_{24}, while apoC-I(35−53) has two, Lys_{37}−Glu_{40} and Glu_{44}−Lys_{48}. Analysis of the calculated three-dimensional structures for apoC-I(7−24) and apoC-I(35−53) indicated that the interatomic distances between all these charged pairs are greater than 8 Å. It can be concluded that there is no significant stabilization of the α-helical structures due to the formation of salt bridges. Therefore, we concur with Segrest who stated that hydrophobic interactions are the main stabilizing force in lipoproteins (Segrest et al., 1992).

CONCLUSION

Biophysical studies of lipid-associating proteins are often conducted in the presence of SDS which serves as a model for a membrane environment (McDonnell & Opella, 1993; Rizo et al., 1993; Henry & Sykes, 1994). Detailed structural analysis of both apoC-I(7−24) and apoC-I(35−53) in the presence of SDS shows that both molecules adopt a conformation best described as a class A_2 amphipathic helix. In both peptides the hydrophobic face occupies approximately one-third of the total surface area. The latter proportion was found to be ideal for penetration of the lipoprotein surface and enzyme activation (Fukushima et al., 1980).

CD data collected by Swaney and Weisgraber (1994) on synthetic apoC-I residues 1−38, 40−57, and 30−57 in the presence of unilamellar vesicles of DMPC show no increase in helical content upon the addition of lipid. They concluded that these apoC-I fragments did not associate with the lipid. While DMPC is often used to represent the monolayer of serum lipoproteins, our results using SDS suggest the latter may be a better biological environment when studying short peptides. We have shown here that apoC-I(7−24) and apoC-I(35−53) form amphipathic helices in the presence of SDS. Binding to lipid is a prerequisite for the activation of LCAT by apoC-I. Therefore, the primary function of residues 7−24 and 35−53 in apoC-I may be as lipid anchors. The conformational changes that occur to the remainder of apoC-I upon the binding of residues 7−24 and 35−53 to lipid may be responsible for the biological functions of apoC-I.

ACKNOWLEDGMENT

We thank Dr. I. Clark-Lewis (University of British Columbia) for kindly providing the peptides. We also thank Drs. W. D. Treleaven, S. J. Dunne, F. D. Sönnichsen (University of Alberta), and K. H. Weisgraber (Gladstone Institute of Cardiovascular Disease) for useful discussions, and B. Ciffelli (Silicon Graphics Inc., Vancouver, BC) and R. Walker (Biosym Technologies Inc., San Diego, CA) for their assistance.

REFERENCES

Albers, J. J., Lin, J. T., & Roberts, G. P. (1979) *Artery 5*, 61−75.

Bairaktari, E., Mierke, D. F., Mammi, S., & Peggion, E. (1990) *Biochemistry 29*, 10090−10096.

Baker, E. N., & Hubbard, R. E. (1984) *Prog. Biophys. Mol. Biol. 44*, 97−179.

Bax, A., & Davis, D. G. (1985) *J. Magn. Reson. 65*, 355−360.

Brasseur, R., Lins, L., Vanloo, B., Ruysschaert, J.-M., & Rosseneu, M. (1992) *Proteins: Struct., Funct., Genet. 13*, 246−257.

Braunschweiler, L., & Ernst, R. R. (1983) *J. Magn. Reson. 53*, 521−528.
Bruch, M. D., Dhingra, M. M., & Gierasch, L. M. (1991) *Proteins: Struct., Funct., Genet. 10*, 130−139.
Clark-Lewis, I., Aebersold, R. A., Ziltner, H., Schrader, J. W., Hood, L. A., & Kent, S. B. H. (1986) *Science 231*, 134−139.
Epand, R. M., Surewicz, W. K., Hughes, D. W., Mantsch, H., Segrest, J. P., Allen, T. M., & Anantharamaiah, G. M. (1989) *J. Biol. Chem. 255*, 4628−4635.
Fielding, C. J., Shore, V. G., & Fielding, P. E. (1972) *Biochem. Biophys. Res. Commun. 46*, 1493−1498.
Fukushima, D., Yokoyama, S., Kroon, D. J., Kezdy, F. J., & Kaiser, E. T. (1980) *J. Biol. Chem. 255*, 10651−10657.
Havel, T. (1991) *Prog. Biophys. Mol. Biol. 56*, 43−78.
Hennessey, J. P., Jr., & Johnson, W. C., Jr. (1982) *Anal. Biochem.*, 177−188.
Henry, G. D., & Sykes, B. D. (1994) *Methods Enzymol. 239*, 515−535.
Holzwarth, G. M., & Doty, P. (1965) *J. Am. Chem. Soc. 87*, 218−228.
Jackson, R. L., Morrisett, J. D., Sparrow, J. T., Segrest, J. P., Pownall, H. J., Smith, L. C., Hoff, H. F., & Gotto, A. M., Jr. (1974) *J. Biol. Chem. 249*, 5314−5320.
Jeener, J., Meier, B. H., Bachmann, P., & Ernst, R. R. (1979) *J. Chem. Phys. 71*, 4546−4553.
Lyu, P. C., Gans, P. J., & Kallenbach, N. R. (1992) *J. Mol. Biol. 223*, 343−350.
Matz, C. E., & Jonas, A. (1982) *J. Biol. Chem. 257*, 4541−4546.
McDonnell, P. A., & Opella, S. J., (1993) *J. Magn. Reson. B102*, 120−125.
Merutka, G., & Stellwagen, E. (1991) *Biochemistry 30*, 1591−1594.
Miller, G. J., & Miller, N. E. (1975) *Lancet 1*, 16−19.
O'Neil, J. D. J., & Sykes, B. D. (1989) *Biochemistry 28*, 699−707.
Osborne, J. C., Jr., Bronzert, T. J., & Brewer, H. B., Jr. (1977) *J. Biol. Chem. 252*, 5756−5760.
Perczel, A., Park, K., & Fasman, G. D. (1992) *Anal. Biochem. 203*, 83−93.
Piotto, M., Saudek, V., & Sklenár, V. (1992) *J. Biomol. NMR 2*, 661−665.
Pownall, H. J., Hu, A., Gotto, A. M., Albers, J. J., & Sparrow, J. T. (1980) *Proc. Natl. Acad. Sci. U.S.A. 77*, 3154−3158.
Rance, M., Sørensen, O. W., Bodenhausen, G., Wagner, G., Ernst, R. R., & Wüthrich, K. (1983) *Biochem. Biophys. Res. Commun. 117*, 479−485.
Redfield, A. G., & Kunz, S. D. (1975) *J. Magn. Reson. 19*, 250−254.
Rizo, J., Blanco, F. J., Kobe, B., Bruch, M. D., & Gierasch, L. M. (1993) *Biochemistry 32*, 4881−4894.
Sarver, R. W., & Krueger, K. C. (1991) *Anal. Biochem. 194*, 89−100.
Scholtz, J. M., Qian, H., Robbins, V. H., & Baldwin, R. L. (1993) *Biochemistry 32*, 9668−9676.
Segrest, J. P., DeLoof, H., Dohlman, J. G., Brouillette, C. G., & Anantharamaiah, G. M. (1990) *Proteins: Struct., Funct., Genet. 8*, 103−117.
Segrest, J. P., Jones, M. K., de Loof, H., Brouillette, C. G., Venkatachalapathi, Y. V., & Anantharamaiah, G. M. (1992) *J. Lipid Res. 33*, 141−166.
Shoemaker, K. R., Kim, P. S., York, E. J., Stewart, J. M., & Baldwin, R. L. (1987) *Nature 326*, 563−567.
Sklenár, V., Piotto, M., Leppik, R., & Saudek, V. (1993) *J. Magn. Reson. A102*, 241−245.
Soutar, A. K., Garner, C. W., Baker, H. N., Sparrow, J. T., Jackson, R. L., Gotto, A. M., & Smith, L. C. (1975) *Biochemistry 14*, 3057−3064.
Sparrow, J. T., Pownall, H. J., Sigler, G. F., Smith, L. C., Soutar, A. K., & Gotto, A. M., Jr. (1977) in *Peptides: Proceedings of the Fifth American Peptide Symposium* (Goodman, M., & Meienhofer, J., Ed.) pp 149−152, Wiley, New York.
Subbarao, N. K., Fielding, C. J., Hamilton, R. L., & Szoka, F. C. (1988) *Proteins: Struct., Funct., Genet. 3*, 187−198.
Swaney, J. B., & Weisgraber, K. H. (1994) *J. Lipid Res. 35*, 134−142.
Sweeny, S. A., & Jonas, A. (1985) *Biochim. Biophys. Acta 835*, 279−290.
Weisgraber, K. H., Mahley, R. W., Kowal, R. C., Herz, J., Goldstein, J. L., & Brown, M. S. (1990) *J. Biol. Chem. 265*, 22453−22459.
Windler, E., & Havel, R. J. (1985) *J. Lipid Res. 26*, 556−565.
Wishart, D. S., Sykes, B. D., & Richards, F. M. (1991) *J. Mol. Biol. 222*, 311−333.
Woody, R. W. (1992) *Adv. Biophys. Chem. 2*, 37−79.
Wu, C., & Yang, J. T. (1978) *Biochem. Biophys. Res. Commun. 82*, 85−91.
Wüthrich, K. (1986) *NMR of Proteins and Nucleic Acids*, Wiley, New York.
Wüthrich, K., Billeter, M., & Braun, W. (1984) *J. Mol. Biol. 180*, 715−740.
Yokoyama, S., Fukushima, D., Kupferberg, J. P., Kezdy, F. J., & Kaiser, E. J. (1980) *J. Biol. Chem. 255*, 7333−7339.

BI942965Z